

Article

Integrated Geospatial and Geophysical Approaches for Mapping Groundwater Potential in the Semi-Arid Bukombe District, Tanzania

Juma N. Kubingwa^{1,2,*}, Edikafubeni E. Makoba² and Kassim Ramadhani Mussa² ¹ Lake Tanganyika Basin Water Board, Kahama Sub-Office, Kahama P.O. Box 471, Tanzania² Department of Geography and Environmental Studies, Sokoine University of Agriculture, Morogoro P.O. Box 3038, Tanzania

* Correspondence: kubingwa@yahoo.com or juma.kubingwa@laketanganyikabasin.go.tz; Tel.: +255-787-465-514

Abstract: The rapid growth of civil societies coupled with population influx due to the artisanal mining industry in the Bukombe district (BD) has triggered a high demand for water resources. The daily consumption of water resources in the district surpasses the supply from available surface water sources. Thus, the situation has raised the demand for groundwater resources as an alternative. Despite the importance of groundwater resources, no current studies have spatially assessed groundwater potential to locate optimal points for borehole development. This study intended to investigate and map the groundwater potential areas (GWPA) in the semi-arid BD using remote sensing (RS), the geographic information system (GIS), and the analytic hierarchy process (AHP) to help local communities access clean and safe water. Rainfall, geology, slope, drainage density, land use/land cover and lineament density were prepared to delineate the map of GWPA. The map was categorized into poor (0.21%), moderate good (51.39%), good (45.70%) and very good (2.70%). Finally, the GWPA map was validated using Vertical Electrical Sounding (VES), 2-D sections and a drilled borehole. The validation results confirmed that the applied approach provides significant results that can help in planning the sustainable utilization of groundwater resources.

Keywords: groundwater potential area; analytic hierarchy process; geographic information system; remote sensing; geospatial and geophysical; Bukombe



Citation: Kubingwa, J.N.; Makoba, E.E.; Mussa, K.R. Integrated Geospatial and Geophysical Approaches for Mapping Groundwater Potential in the Semi-Arid Bukombe District, Tanzania. *Earth* **2023**, *4*, 241–265. <https://doi.org/10.3390/earth4020013>

Academic Editor: Hossein Bonakdari

Received: 26 January 2023

Revised: 22 February 2023

Accepted: 23 February 2023

Published: 5 April 2023



Copyright: © 2023 by the authors. Licensee MDPI, Basel, Switzerland. This article is an open access article distributed under the terms and conditions of the Creative Commons Attribution (CC BY) license (<https://creativecommons.org/licenses/by/4.0/>).

1. Introduction

Globally, water is recognized as a basic irreplaceable need of human beings. Its accessibility, however, is a major challenge, especially in developing countries [1], because of the dwindling surface water sources due to climate change and anthropogenic pollution [2–5]. In recent years, climate change, rapid population growth and surface water losses within the conveying pipes during transportation from sources to storage reservoirs have made groundwater the most demanded resource [6,7]. Moreover, some communities perceive the quality of groundwater to be better and more reliable than other sources of water for domestic uses [6]. Thus, it is important to locate dependable sources of groundwater supply in all climatic regions across the world [8].

Demographic data show that about 11% of the world's population, particularly in Sub-Saharan Africa and Oceania, do not have access to clean and safe water [9]. The majority have aligned themselves to an alternative and cost-effective source, which is groundwater [10]. The lack of adequate hydrogeological and updated geospatial data in place to identify groundwater potential areas has led to the drilling of boreholes and the digging of wells in areas where groundwater potentiality is suboptimal [11–13].

Economic water scarcity is a common problem in developing counties such as Tanzania [3,4]. About 25% of Tanzania's population depends on groundwater sources for domestic and

other uses [14]. In spite the significance of this concern, groundwater resources are not thoroughly explored in terms of aquifer extent, aquifer characteristics and water quality to sufficiently cater to users [15,16], and the most affected areas where groundwater is poorly explored is the western part of Tanzania. As a result, individuals, communities and institutions have decided to pass on important indigenous knowledge on exploiting and managing shallow aquifers [17]. Due to current climate variability and change, high levels of resource exploitation, increased urbanization and population growth, the determination of groundwater potential areas in developing countries, particularly in semi-arid areas, is inevitable [18]. However, this is challenging as it needs reliable information for locating the boreholes within a groundwater potential area [18–20].

In semi-arid region such as the Bukombe district in western Tanzania, groundwater is the major source of water for domestic uses [21]. Due to water scarcity, groundwater projects initiated by the government and NGOs to narrow the water supply gap experienced failure a few years after inauguration. This was largely attributed to the paucity of technical knowledge in the field of satellite data use that hampered the assessment of tangible groundwater potential areas [3]. Research conducted by SMEC (2015) identified Bukombe as one of the areas in the Malagarasi catchment with severe groundwater risk. Furthermore, their study revealed that Bukombe is the area where groundwater recharge takes place and is proposed to be legally protected to safeguard not only the welfare of the people but also the Malagarasi-Muyovosi Ramsar Site [15]. However, the spatial distribution of the groundwater potentiality, aquifer characteristics and groundwater quality are vaguely known.

Therefore, this research intended to assess groundwater potential areas in the Bukombe semi-arid area using geospatial and geophysical approaches which digitally demarcated and categorized the area for further groundwater development. Our findings agree with results from previous researchers which demonstrated that RS and GIS provide potentially powerful tools to study groundwater resources [22–24].

2. Materials and Methodology

2.1. Descriptions of Study Area

2.1.1. Location and Accessibility

Bukombe is one of the districts in the Geita region, northwest Tanzania, covering an area of about 8000 sq. km between latitudes 3.11–4.47° S and longitudes 31.15–32.167° E (Figure 1). The district is bordered to the south by the Kaliua district, to the west by the Kibondo district and to the north by Biharamulo, Chato and Geita districts; in the eastern part, it is bordered by Mbogwe and Kahama districts. A large area in the southern part falls under the Kigosi National Park (Figure 1). The study area is accessible through the tarmac road of the Isaka-Rusahunga highway in almost all town centers. Most of the villages are accessible through rough roads in both wet and dry seasons.

In 2012, the population of the Bukombe district was 224,542 [25]. It is projected to be 333,934 in 2025 using the population projection model as per Equation (1).

$$P_f = P_p(1 + gr)^t \quad (1)$$

where P_f , P_p , gr and t are the future population, previous population, growth rate and time in years, respectively (<https://www.youtube.com/watch?v=ygMCKsb4aAU>, accessed on 25 January 2023).

The land use in the Bukombe district includes the forest where there is the Kigosi National Park and the community and individual forest reserves [26], along with agricultural land, especially paddy pans and corn cultivated areas. Settlement areas ranging from towns to village housing are also present. The curve number for town centers in general is higher than for villages as a result of accelerating surface runoff. The mining industry also accounts for a small portion of land use in the district.

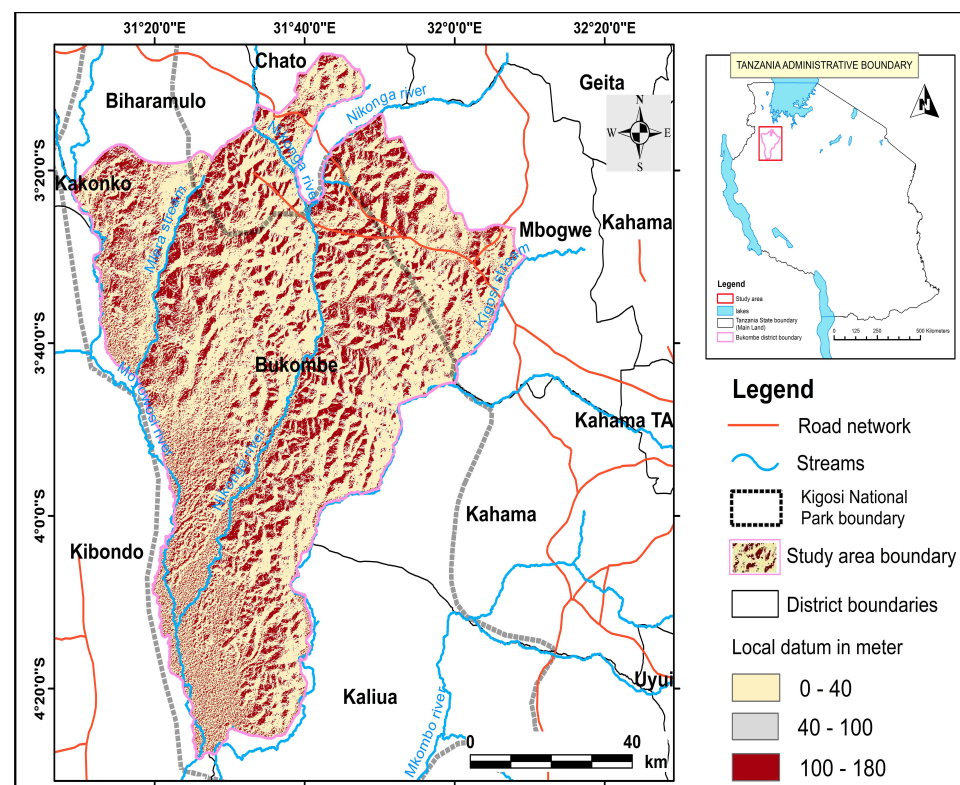


Figure 1. Population, land use and water demand.

Water demand in the Bukombe district is not explicitly displayed but rather could be inferred from the water demand, estimated on the Malagarasi catchment of which the Bukombe district is a part. SMEC (2015) estimated the water demand in the Malagarasi catchment as 1299 MCM/year in 2015, 1437 MCM/year in 2025 and 1704 MCM/year in 2035 [15]. With a simple areal- and population-based ration, Bukombe's water demand can be downscaled to 208 MCM/year in 2025 that will be used for domestic purposes, irrigation, tourism, wildlife, mining, industry, livestock keeping and recreation. According to BDAR 2021, the district is planning to have 5 recreation sites and 2 sports grounds; develop 1850 ha for irrigation in Bugelenga, Mjimwema and Nyampangwe, where 250 ha and 100 ha in Bugelenga and Mjimwema, respectively, are locally being irrigated; and raise the water supply coverage that will cater to over 130 lodges, industries, mining activities, livestock, etc. [26].

2.1.2. Climate

The climate of the study area is that of a tropical savannah with distinct rainy and dry seasons [16]. The district experiences a unimodal rain pattern with total annual rainfall ranging between 600 and 1000 mm [15]. Rainfall occurs between October and May with a short break in January or February [27]. The rest of the months are the dry season [15]. The temperature ranges between 20 and 35 °C, with annual evapotranspiration of 1600 mm per year.

2.1.3. Hydrogeological Settings

Based on Tanzania's water basins, the Bukombe administrative district falls under the Lake Tanganyika Basin, the second largest basin after the Rufiji Basin, with an area of 160,426 sq. kilometers (Figure 2a,b). BD lies at the upper Malagarasi catchment consisting of three subcatchments made of the Mlera, Nikonga and Kigosi rivers [16]. It is dominated by NE–SW, N–S and NW–SE lineaments that might have led to the formation of the Mlera and Nikonga rivers in the middle, the Moyowosi river in the west and the Kigosi stream in the east (Figure 1). The Moyowosi and Nikonga rivers are perennial, whereas the Mlera and Kigosi rivers are ephemeral in their upstream but become active as they approach the

confluence with the Moyowosi river. Groundwater potentiality is mainly dependent on geological structures and alluvial basins (Figure 3). The available boreholes in the study area are located in an alluvial basin (Figure 3).

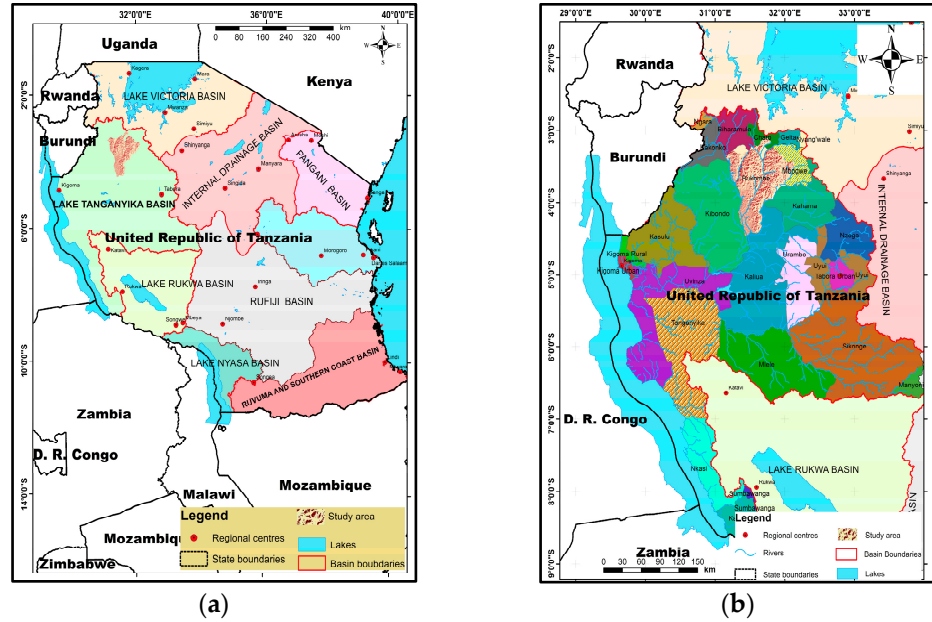


Figure 2. (a) The United Republic of Tanzania showing the nine hydrological basins. (b) Lake Tanganyika Basin with its 26 districts, including BD.

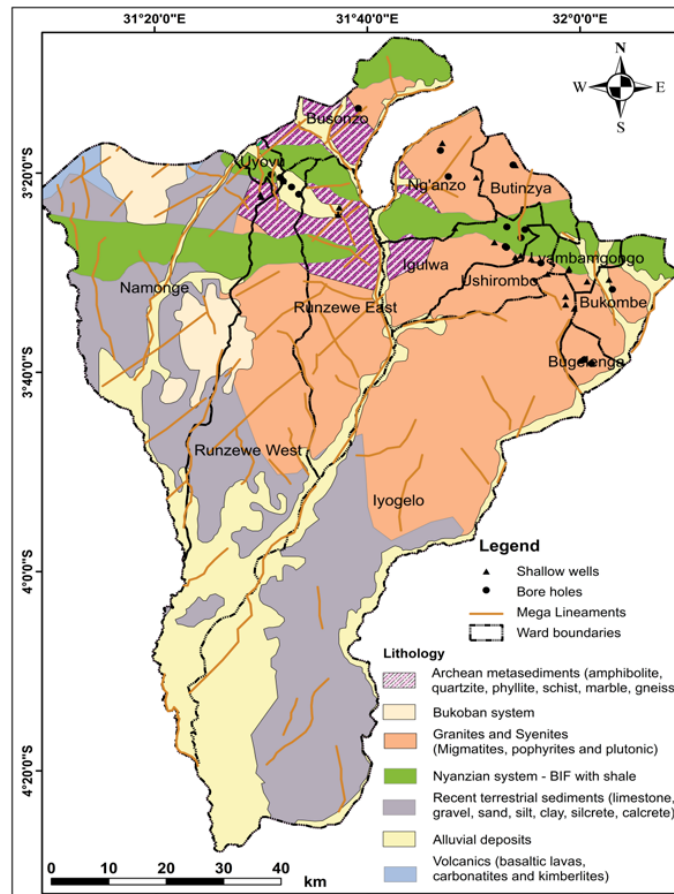


Figure 3. Geological map of the study area (extracted from Barth 1990, Taylor 2009 and SMEC 2015).

2.1.4. Geological Setting

The Bukombe district is part of the Lake Victoria Gold Field (LVGF). LVGF is the area comprising large gold mines and has been documented as an important site for gold mining and exploration in East Africa [28,29]. Rocks within the gold fields have been subdivided into the Nyanzian System and the Kavirondian System. The Nyanzian System comprises an assemblage of mafic metavolcanics, chemical sediments (oxide and silicate facies iron formation) and lesser epiclastic sediments [30]. Minor ultramafic and felsic volcanics plus volcano clastics form basal and capping members, respectively, of the largely tholeiitic volcanic pile. These Nyanzian rocks are unconformably overlain by the Kavirondian System, which consists of epiclastic sediments and minor tuffs. Both systems are intruded by large granitic plutons. The Banded iron formation and Banded ferruginous chert are narrow zones that overlie the basic volcanic piles [30]. Visual observations by the researcher confirmed the weathered sedimentary rock locally known as the laterites in both Katente and Bulangwa wards (Figure 3).

2.2. Types of Data and Data Collection Procedures

Geospatial data collection and processing included the satellite image and digital elevation model, the total annual rainfall (TAR) data and the geological map. Fieldwork included a geophysical survey for subsurface lithological analysis.

The Digital Elevation Model (DEM) was downloaded from the Earth Explorer website (Shuttle Radar Topography Mission (SRTM-DEM)) of 30 m resolution (<https://earthexplorer.usgs.gov>, (accessed on 25 January 2023)). The satellite images (20% cloud cover) were downloaded from Landsat8, particularly using the OLI sensor data. Three tiles were needed, 171–063, 172–062 and the 171–062, where the first and last numbers represent the path and row of the satellite.

Conventional data were individually handled in accordance with their respective standard procedures. Rainfall data, for example, from 21 rainfall stations were collected from Lake Tanganyika Basin Water Board, Kahama Sub-Office and remotely from Lake Victoria Basin Water Board. The geology maps from the Tanzania Geological Survey were collected in picture mode quarter degree sheets 44, 45, 60, 61, 76 and 77.

Geophysical data were collected in two phases; the first phase was 2-D and the second phase was 1-D. In the 2-D geophysical survey, a 32-channel McOhm Profile-4 resistivity system utilizing a pole dipole electrode array type was used to acquire profiles each 280 m long with an electrode interval of 10 m. Pole dipole array enables one to obtain the quantitative depth, lithological information and resistivity information below the measurement station [31]. Fourteen profiles were measured at the locations of Ilyamchele, Bulangwa, Katente, Shikalibuga, Roman Catholic Mission and Runzewe.

The vertical electrical sounding (1-D) resistivity measurements were carried out in the anomalous points interpreted from the 2-D pseudo-sections. It utilized ABEM Terrameter LS with Schlumberger configuration at the minimum and maximum current electrode spacing (AB) of about 3 and 600 m, respectively, which is suitable for a subsurface investigation depth of about 300 m [13,32]. A total of 80 VES stations were included in the study area and out of the 2-D profiles aiming at widening the scope of comparing the two approaches.

2.3. Data Analysis

2.3.1. Geospatial Data Analysis

The preparation of thematic maps and later the groundwater potential area map was entirely dependent on GIS software. A total of six thematic layers were generated from DEM, satellite images, climatological data and geology as described below. The DEM from the Shuttle Radar Topography Mission generated two thematic maps, one of the drainage density and one of the slope (Figure 4).

Drainage density was generated by following sequential algorithms: fill, flow direction, flow accumulation, threshold dataset, stream order and stream to feature, then drainage density. The slope is a measure of elevation change and termed as a topographic

parameter [33]. The slope was produced in GIS through the conversion of DEM into a slope dataset and reclassification into five classes according to Van Zuidam, who divided the slope as follows: 0–2% flat, 2–15% moderate, 15–25% moderate steep, 25–40% steep and greater than 40% very steep [33]. The rainfall map of the study area was prepared by interpolating the TAR from 21 stations (Appendix C). The data were processed using GIS and interpolated using Kriging interpolation to produce the rainfall map (Figure 5b).

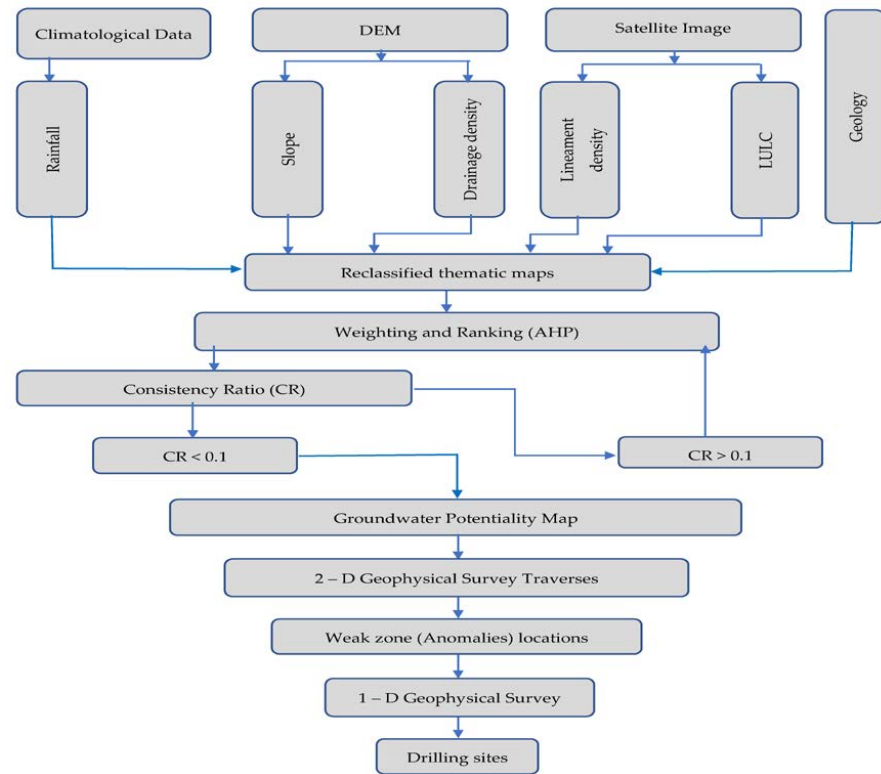


Figure 4. Framework showing the procedures involved during data acquisition and analysis.

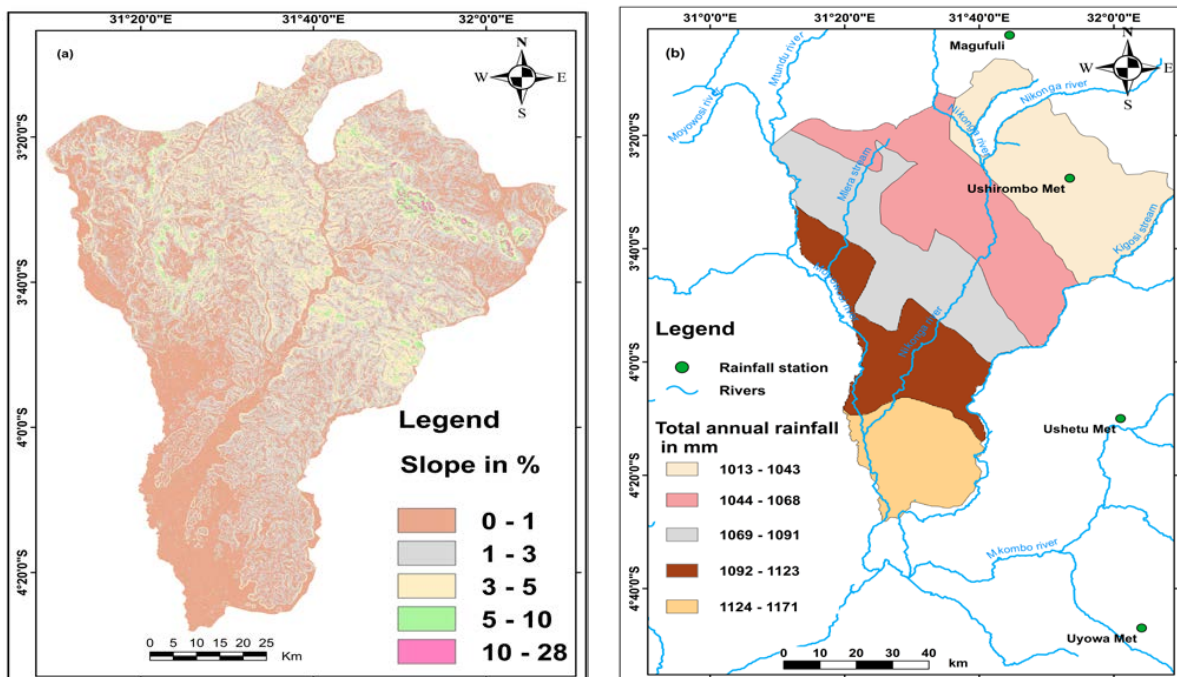


Figure 5. BD map showing spatial distribution of (a) slope and (b) total annual rainfall.

Three satellite images were used to classify the study area into different types of land use and land cover (LULC). The procedures and steps undertaken were image enhancement through dark object subtraction DOS, conversion into false color composite FCC, mosaicking and clipping into study area jurisdiction. Training samples’ definition was the next step after clipping, during which macro and micro classes were developed [34]. Finally, the five LULCs (water body, forest, built up, agricultural land and the bare land) were generated through interactive supervised classification.

The lineament density map was generated from mosaicked satellite image in QGIS. A single red band was selected, from which hill shades of azimuth angles 45°, 135°, 225° and 315° were developed. A polyline layer was also prepared, onto which lineaments were manually digitized from the hill shade layers at a 1:100,000 scale [35]. Cultural and/or manmade linear features such as roads, canals and rail lines were eliminated by projecting the lineament layer onto Google Earth to ensure that all the digitized lineaments are purely geological features [35]. The final lineament density map was created.

The geological maps from the Tanzania Geological Survey (QDS 44, 45, 60, 61, 76 and 77), the Lake Tanganyika Basin geological map from SMEC report and the LVGF map were used to extract geological formations in the study area [15,30]. A total of six geological formations were identified (Figure 3): basalt, recent sediments (limestone, calcrete, gravel, sand, silt and clay), alluvial deposit, granites, metasediments of Archean age (phyllite, schist, gneiss, amphibolite and marble) and the Nyanzian Kavirondian in the form of banded iron formation.

Thematic layers were then input into AHP excel software for pairwise comparison weight calculation. At this stage, each thematic layer was compared to other layers one at a time to choose which of the two is more important than the other with regard to groundwater potentiality. The choices made assigned ranks to themes and their classes from 1 (equally important) to 9 (extremely important) depending on how important a factor is over the others, as per Saaty’s (1980) classification [10,36] as Table 1 elaborates. Of equal importance, the consistency ratio was monitored at all times, making sure it was an acceptable value of at most ten percent (see Appendix A) [12].

Table 1. Preference scale for two parameters in AHP (Saaty 1980).

Scale	Intensity of Importance	Explanation
1	Equally	Two activities contribute equally to the objective
3	Moderately	Experience and judgment slightly to moderately favor one activity over another
5	Strongly	Experience and judgment strongly or essentially favor one activity over another
7	Very strongly	An activity is strongly favored over another and its dominance is shown in practice
9	Extremely	The evidence of favoring one activity over another is of the highest degree possible of an affirmation
2,4,6,8	Intermediate values between two judgments	Used to represent compromises between the preferences in weights 1, 3, 5, 7 and 9

Ranks for aggregates of each theme were set based on the literature, field experience and groundwater science expertise [37]. The thematic layers in raster format were overlaid using the weighted overlay command as per the following equation to generate groundwater potential area (GWPA) [12,21,38]:

$$GWPA = \sum_1^n ((w_{tm}) \times (r_{tm})) \tag{2}$$

where w_{tm} is the weight of the thematic factor and r_{tm} is the scale value or rank each aggregate is given by the researcher. Detailed clarification on weight values and ranks for this study are provided in Appendices A and E.

The generated GWPA was used to select potential areas for conducting geophysical measurements. The selection of the traverses during the resistivity survey was based

on geomorphological settings, indigenous historical narration and the existence of local water sources, aiming at capturing key areas that seemed to be prominent for groundwater development. The 2-D survey was conducted first to map the subsurface geology using Marcohm Profile 4 machine followed by the 1-D Terrameter Ls on promising points for confirming and locating drilling sites (Figure 4).

2.3.2. Geophysical Data Analysis

Modeling and inversion of the 1-D resistivity data were performed using IP2WIN/DCINV software to generate resistivity models with charts and tables. The 2-D resistivity data were analyzed using RES2-DINV software to produce sections' interpretation of geological layers in relation to groundwater occurrence. The final output was the identification of the number of aquifers, depth to the aquifer, thickness of the aquifer and resistivity of the aquifer [39].

3. Results

This section portrays two main types of results: the geospatial results and the geophysical results. The geospatial part includes thematic layers which were integrated to produce the GWPA map. The geophysical part accounts for both VES data and 2-D data in terms of resistivity charts and resistivity sections, respectively. The latter part was carried out for the sake of confirming the validity of the former part's results. Lastly, the general conclusion was made that delineated groundwater potential areas can be used to undertake further water projects.

3.1. Geospatial Results

3.1.1. Slope

Geomorphology in any particular area governs the movement of water. Steep slopes promote runoff, while topographical depressions favor infiltration [21]. The slope, like other themes, plays a significant role in groundwater recharge leading to groundwater potentiality. With reference to Van Zuidam's slope classification, BD has only two classes: flat and moderate. However, the slopes in the study area were categorized into five classes: (i) very low slope (<1%), (ii) low slope (1 to 3%), (iii) medium slope (3 to 5%), (iv) high slope (5 to 10%) and (v) very high slope (>10%). With reference to Figure 5a, a large area falls under low and very low classes, accounting for more than 60% of the entire area. This means that a large amount of water from rain is given ample time to infiltrate, hence recharging the aquifer and increasing the groundwater potentiality, if and only if other factors remain constant.

3.1.2. Rainfall

Rainfall plays major role in recharging groundwater. Therefore, areas with higher rainfall are generally considered as potential zones for groundwater exploitation. The rainfall map of the study area (Figure 5b) was divided into five classes: (1) low rainfall zone with rainfall less than 1043 mm, (2) moderate rainfall zone with rainfall between 1043 and 1068 mm, (3) good rainfall zone with rainfall between 1068 and 1091 mm, (4) very good rainfall zone with rainfall between 1091 and 1123 mm and (5) excellent rainfall zone with rainfall more than 1123 mm. The northeast part receives the least amount of rainfall; the precipitation sequentially increases through to the far southwest end, which has an excellent amount of rainfall (Figure 5b). This is attributed to the Kigosi National Park, which accounts for a large portion of the district. The range of rainfall is not that substantial, and areal percent for all classes are 23.95%, 24.39%, 22.10%, 16.57% and 12.99%, respectively.

3.1.3. Land Use/Land Cover

Land use/land cover of an area is largely governed by the groundwater resources and, at the same time, plays an important role in controlling these resources. It influences

many hydrogeological processes in the water cycle such as evapotranspiration, infiltration, surface runoff, etc. [40,41]. In the forest and agricultural land, runoff is generally less prevalent and infiltration is more common, whereas, in settlement areas and other built up parts such as tarmac roads, the rate of infiltration usually decreases due to the high curve number possessed by such areas.

Therefore, agricultural land and vegetation cover area were ranked higher than built-up area [38]. In the Bukombe district in particular (Figure 6a), a major portion of land use is forest, covering 5984.133 sq. km (74.3%), along with bare land covering 1456.541 sq. km (18.1%), agricultural land covering 387.404 sq. km (4.8%) and water and settlements each covering 1.4% with areas of 116.506 sq. km and 109.45 sq. km, respectively. The correctness of these results was checked by creating the classification confusion matrix, as displayed in Table 2. Recent research pointed out that the minimum acceptable accuracy assessment is 70% [42]. The accuracy assessment of this research is more than sufficient, as given in Table 2.

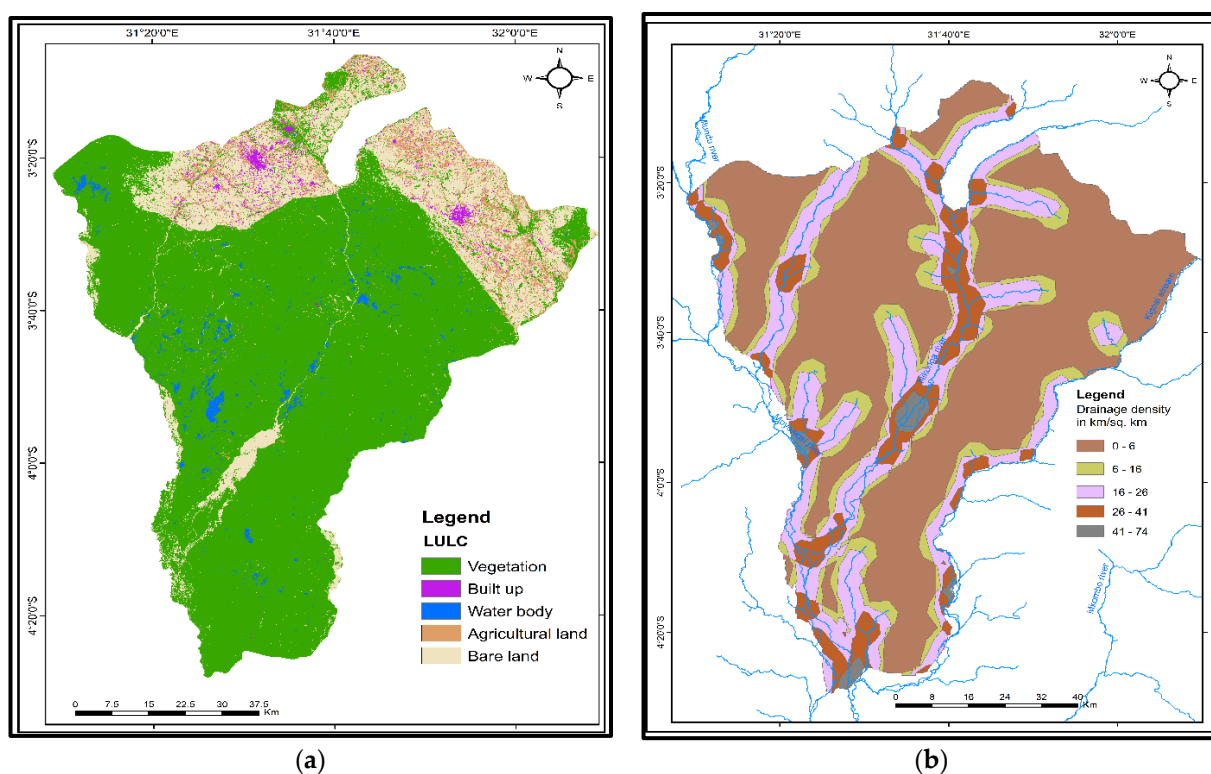


Figure 6. BD map showing coverage of (a) land use/land cover and (b) drainage density.

Table 2. Interactive supervised classified land use/land cover confusion matrix.

Class Value	Vegetation	Built-Up	Water Body	Agricultural Land	Bare Land	Total	User Accuracy	Kappa
Vegetation	98	0	1	1	0	100	0.98	0
Built-Up	2	52	5	23	18	100	0.52	0
Water Body	10	0	90	0	0	100	0.9	0
Agricultural Land	0	1	1	94	4	100	0.94	0
Bare Land	12	0	0	0	88	100	0.88	0
Total	122	53	97	118	110	500	0	0
Producer Accuracy	0.80	0.98	0.93	0.80	0.8	0	0.84	0
Kappa	0	0	0	0	0	0	0	0.81

3.1.4. Drainage Density

The quantification of drainage density and its types leads to runoff, infiltration, relief and permeability information acquisition [38]. It also reflects the proximity of spacing of streams as well as surface characteristics [43]. Further, drainage patterns give information

related to surface materials and subsurface formation. For instance, dendritic drainage indicates homogenous rocks, whereas trellis, rectangular and parallel drainage patterns are suggestive of structural and lithological controls [38]. The Bukombe district in particular is characterized by a dendritic drainage pattern. Geospatial analysis categorized five classes of drainage density: very low, low, medium, high and very high, with areal percentages of 58.2%, 15.6%, 17.9%, 6.7% and 1.6%, respectively (Figure 6b). With these data, Bukombe can be presumed to be gently sloping to flat land that promotes more infiltration. It is of a lower drainage density, which encourages more groundwater potential than high-drainage-density regions [22,44]. Low drainage density yields a coarse drainage texture and high drainage density leads to a fine drainage texture [44]. So, drainage density has an inverse effect on permeability. Therefore, it is an important feature in evaluating groundwater potential zones.

3.1.5. Lineament Density

The linear faults, accompanied by the fissure, provide space for the occurrence of groundwater [45]. In the stratum with the same lithology, the intersection of the faults leads to the development of the fissure, which tends to be the groundwater enrichment zone with the connectivity enhancement [6]. The linear structures extracted from Landsat 8 OLI images with the aid of the GeoTrace plugin in QGIS led to the formation of five lineament density classes in the study area (Figure 7a). The very low class has an area of 3358.585 sq. km (41.70%), the low lineament has an area of 1184.481 sq. km (14.71%), the medium lineament class has an area of 1401.553 sq. km (17.40%), the high lineament class has an area of 1605.99 sq. km (19.94%) and the very high lineament class has an area of 503.439 sq. km (6.25%). With these lineament data, structural controlled formations in the Bukombe district are limited.

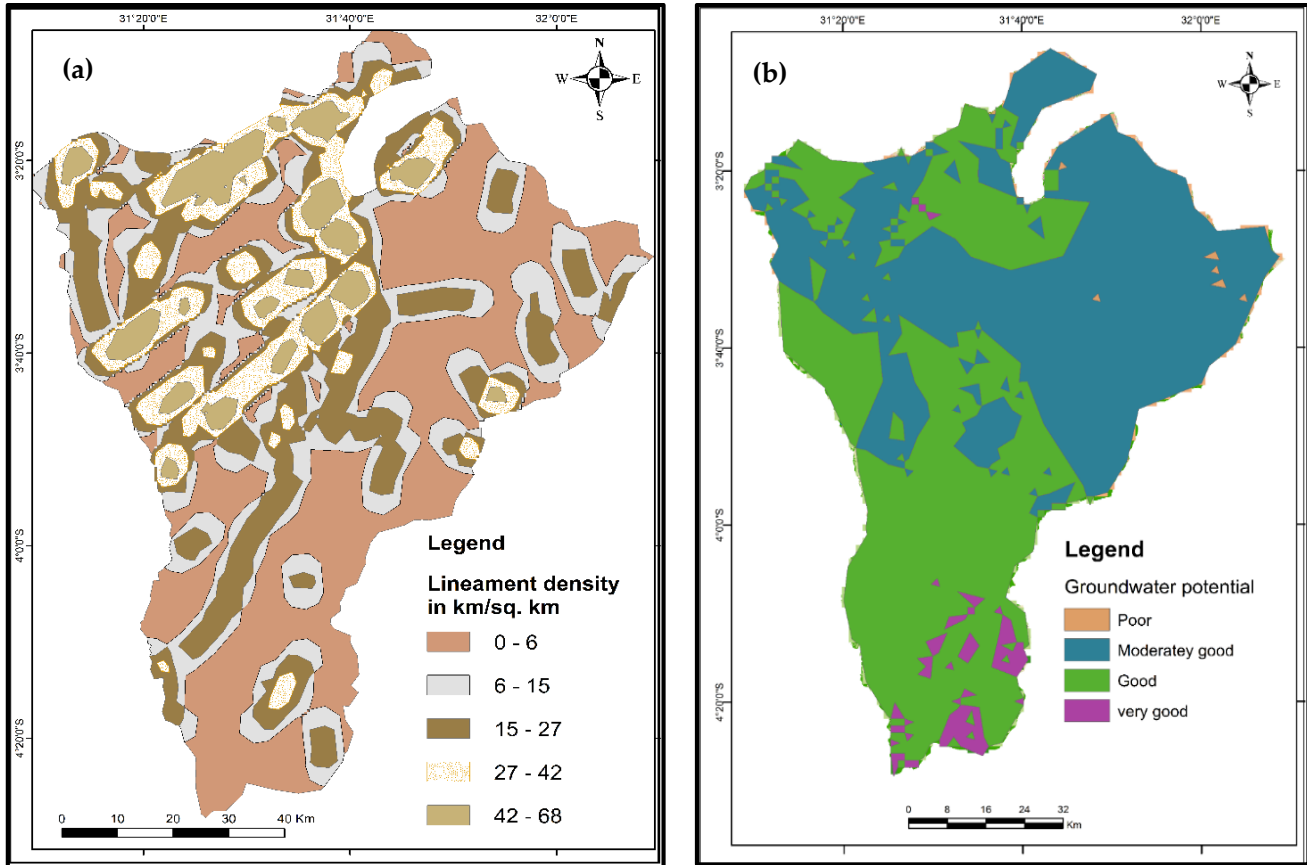


Figure 7. BD map displaying (a) lineament density and (b) delineated groundwater potential areas.

3.1.6. Geology

Geological formations are vessel-like features that hold groundwater in their pore spaces. The knowledge of how these earth materials formed and the evolution they have undergone opens understanding of the distribution of geologic parameters such as permeability and porosity [46]. Higher porosity contributes to higher groundwater storage and higher permeability contributes to higher groundwater yields [47].

The study area comprises a variety of geological formations (Figure 3), including metasediments of Archean age with areal coverage of 7.6%, and the granites and syenites family (41.72%). They are not intensively weathered, which hinders the infiltration of meteoric water, leading to low groundwater recharge. Recent terrestrial sediment accounts for 45.61% of the total area. Such areas have good hydraulic conductivity due to the presence of loose and coarse-grained material. The Nyanzian accounts 3.16% of the total area. The volcanic lava in the northwest corner of the study area has an areal extent of 1.92%. Outcrops of banded iron formation currently serve most of the shallow dug wells and springs for various uses. Groundwater occurrence is higher in metasediments (Figure 7b) and the least in granites due to their aforementioned properties. The degree of metamorphism and weathering, the presence of geologic structures such as folds, non-conformability and faults escalate significant storage of water.

3.1.7. Groundwater Potential Map

The groundwater potential map area is presented in Figure 7b. Groundwater potentiality was demarcated, ending up with four areas (Table 3): poor, moderate, good and very good. The area with very good potential covers 215.56 sq. km, equivalent to 2.70% of the total district area. The spatial location of this area is mostly in the Kigosi National Park, with a few portions in the western part of Runzewe and Uyovu wards, as per Figure 7b. The good category lies mostly in the forest zone and partly in Runzewe west and Runzewe east wards. The potentiality demarcation by the software concurs with the true situation found on the ground, that the aforementioned areas have better groundwater potentiality than the eastern part of the district. The area with good potential covers 3649.70 sq. km, equivalent to 45.70%.

Table 3. Groundwater potential area categories.

No.	Groundwater Potential Area	Area Coverage in sq. km	% Area
1	Poor	16.74	0.21
2	Moderate	4104.07	51.39
3	Good	3649.92	45.70
4	Very good	215.56	2.70

The moderate groundwater potential zone is the largest area of all, occupying most of the residential area in the east, north and west. It covers an area of 4104.07 sq. km, corresponding to 51.39% of the total area. The poor groundwater potential zone is the smallest category, with an area of 16.74 sq. km, equal to 0.21% of the total area, and it appears as a spot on the map (Figure 7b). This area lies in the granitic zone, where little water is able to percolate into ground aquifers. The central to western part corresponds to alluvial plains and lacustrine sediments, which coincide with the low-slope and high-lineament areas.

3.2. Geophysical Results

3.2.1. Vertical Electrical Sounding Results

The inversion of the 80 VES measurements was calibrated using control VES data that were taken from existing boreholes. The results and the inferred interpretative curves (Table 4 and Appendix D) reveal that the subsurface structure of the study area comprises a complex sequence of lithological layers.

Table 4. VES descriptive statistics showing resistivity, layer thickness and layer depth of different stratigraphic formations.

Layer	Parameter	Minimum	Maximum	Mean	Std. Deviation
First layer	Resistivity 1	14.50	110,000.00	5426.83	23961.36
	Thickness 1	0.00	2.50	0.92	0.50
	Depth 1	0.20	2.50	0.93	0.49
Second layer	Resistivity 2	1.20	89.10	20.80	22.42
	Thickness 2	0.30	8.40	2.34	2.54
	Depth 2	0.60	10.90	3.25	2.85
Third layer	Resistivity 3	2.30	93.90	26.17	29.84
	Thickness 3	1.20	177.30	24.39	40.47
	Depth 3	1.80	99.90	20.04	21.97
Fourth layer	Resistivity 4	3.50	167,500.00	85.50	5.58
	Thickness 4	0.50	30.00	15.34	10.59
	Depth 4	4.80	36.40	23.95	13.34
Fifth layer	Resistivity 5	83.30	6804.00	3163.93	2386.90
	Thickness 5	10.00	10.00	10.00	
	Depth 5	14.80	14.80	14.80	
Sixth layer	Resistivity 6	2.00	2.00	2.00	
	Thickness 6	18.60	18.60	18.60	
Seventh layer	Resistivity 7	33.40	33.40	33.40	
	Thickness 7	1085.00	1085.00	1085.00	

The number and the sequence of different layers vary from one site to another (Figure 8), reflecting the lithological complexity and heterogeneity. The succession of lithological layers and the vertical distribution of resistivity values, as shown in interpretative curves, allow us to distinguish two patterns of subsurface structures, namely the weathering profile of Precambrian basement rocks and the presence of alluvial deposits. The sequence of interpreted lithological layers illustrated that the subsurface is composed of three to seven lithological layers with a generally high–low–highest depth trend of resistivity values (Appendix D).

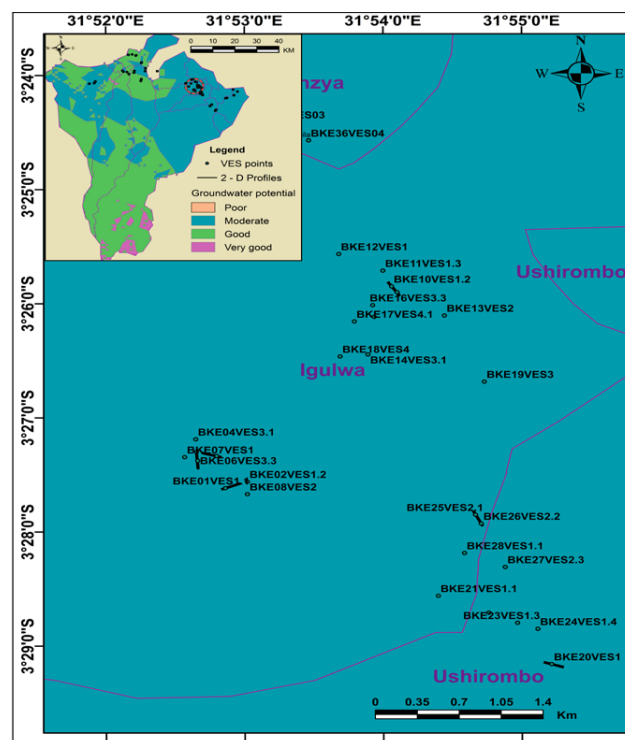


Figure 8. Cont.

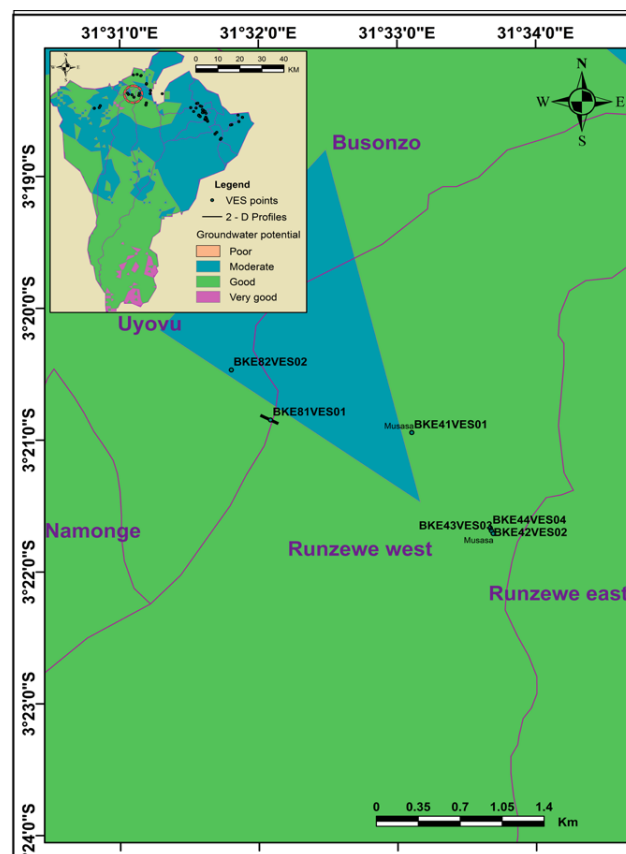


Figure 8. BD maps showing VES and 2-D locations in different GWPA.

The VES measurements undertaken in the study area were dominated by several curve types, of which 40% belong to KH type, 19% fall under HA type, 15% were categorized as H type and 6% are of QH type. AA, KHKH, QHKH, HAA, AKH, QHKA, HKHA, KAA, KHA, QKH, QH and HAKH share the remaining percentage. Experience through practical fieldwork conducted by the researcher in the study area revealed that H and/or other combined types with H as one of the aggregates and with resistivity less than or equal to $100 \Omega\text{m}$; such VES sections have more than 70% of striking groundwater.

The uppermost layer of almost all VES measurements conducted has resistivity above $100 \Omega\text{m}$, suggesting the presence of the duricrust, especially laterite with thickness ranging from ~ 0.4 m to ~ 1.5 m. The second layer is relatively thicker than the first layer (~ 8.4 m thick), with resistivity of about $20 \Omega\text{m}$ corresponding to loam soil intercalated with fine sand. It is within this formation where shallow wells are tapped. The third layer (~ 24 m, thick) with the resistivity of $26 \Omega\text{m}$ reveals more moisturized clays. The fourth layer (~ 23 m) is characterized by resistivity of about $85 \Omega\text{m}$, suggesting the presence of fresh groundwater formation hosted in gravels, sand and alluvial sediment formation. The fifth through seven layers are characterized by resistivity above $1085 \Omega\text{m}$, suggesting massive felsic rock (Table 4).

3.2.2. Two Dimensional (2-D) Geophysical Survey Results

The two-dimensional results tested on several points of the study area are pictorially presented in Figure 9. Examinations showed that the sections possess at least three layers, starting with the upper thin layer with resistivity between 250 and $300 \Omega\text{m}$. Its thickness ranges between 1 and 10 m with discrete to continuous extension in different locations. It represents the lateritic layer of the weathered BIF, as experienced during the field visit. The second layer is covered by the aquifer layer in most of the VES measurements undertaken, having low resistivity ranging from 20.0 to $100 \Omega\text{m}$ with the greatest thickness in the western part of the study area (Figure 9C) and the least (Figure 9A) to almost no thickness

in the eastern part (Figure 9B). It is marked by the blue water drop symbol in Figure 9. Currently, operating boreholes tap their water in this layer; for example, the Bulangwa and Katente boreholes are owned by the Ushirombo town water supply, Isemabuna is used for the Butinzya water scheme, and Kazibila and Nuru boreholes are for the Runzewe town water supply scheme. The third and fourth layers cover the slightly hard to massive granite with resistivity greater than 250 Ω m, marked by a gray water drop symbol.

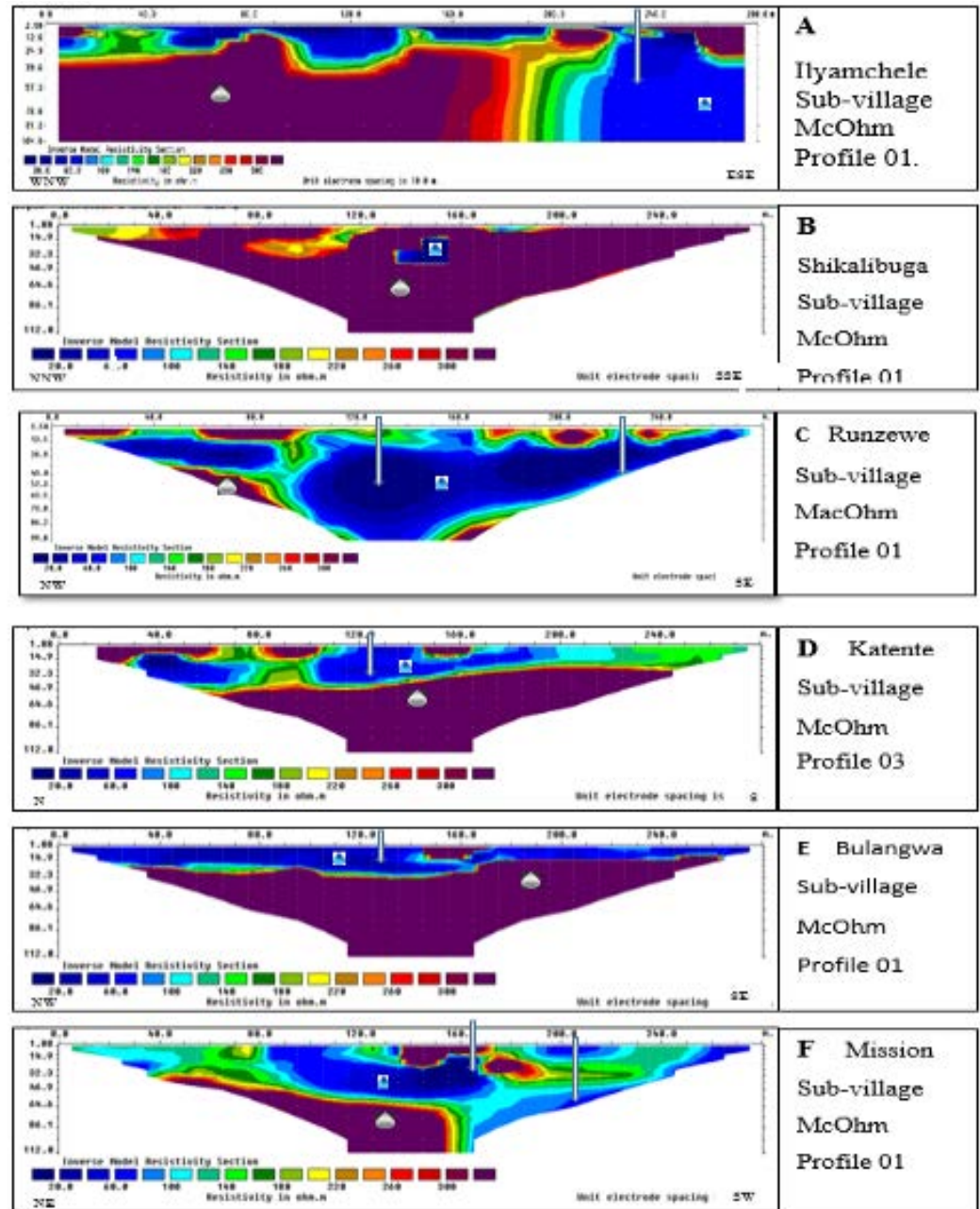


Figure 9. Two-dimensional sections (A–F) from different locations showing saturated formation, hard rock and structural features (fault or fracture).

Again, the eastern part comprises profiles (Figure 9A,B,D,E) with thicker massive rock than the western part (Figure 9C), concurring with the geological map, which shows the existence of the granite formation in those particular areas. Structural controlling groundwater occurrences were marked by thick downward-facing arrows (Figure 9A–F), suggesting points prone to groundwater development.

4. Discussion and Result Validation

4.1. Discussion

Demarcation of groundwater potential areas of the Bukombe semi-arid complex basement aquifer has been undertaken using both geospatial and geophysical methods with the aid of remote sensing and GIS. An overall perspective is that rainfall, geology, lineaments and land use/land cover pattern play important roles in influencing groundwater potentiality (Appendix A). Past studies [22,24,45] concluded more or less similar findings, with slight differences. Allafta pointed out lithology, geomorphology, land use/land cover, rainfall and lineament density as the main controlling factors for groundwater recharge and/or groundwater potentiality; Murasingh suggested that slope, lineament density and drainage density are the major factors influencing groundwater potential, with land use/land cover having medium influence and soil and geomorphology having the least; Rahmat et al. posited that rainfall, lithology and lineament density be the most influential factors for groundwater potentiality. Such conclusions are in line with the results of this study in most cases. In this study, however, it was found that rainfall, geology, lineament and land use/land cover, in order, are the most important factors. Deviations from previous findings are due to a number of reasons, e.g., the number and type of thematic layers used, the difference in aridity index of the study area and the type of geology/lithology of the study area, to mention few.

Locations and areal size of the very good groundwater potential area in the study are relatively bigger than those of the areas identified as poor by 2.5%. The good groundwater potential areas are principally characterized by high rainfall, gentle to flat slopes, a good distribution of lineaments leading to high lineament density, forested land cover and geological formations with good hydraulic conductivity due to the presence of loose and coarse-grained material which allows infiltration and recharge of the aquifer [7,24,38,41,43–45,47]. Meanwhile, the poor groundwater potential area is characterized by high drainage density, low rainfall, few to no lineaments and steep slopes, as reported by other researchers [45].

Geology and rainfall as portrayed by AHP decision support played important roles in divulging the groundwater potential areas. Lineament, in particular, was the third most important theme in this study, concurring with note put forth by recent researchers on providing important information on subsurface fractures which control the movement and storage of groundwater [48]. Land use/land cover is the second least important, and drainage density and slope follow with about 4% weight each (Appendix A). Bukombe district aquifers with poor groundwater potential areas coincide with massive granitic formation, low rainfall, few lineaments and high-drainage-density areas, which accelerate high runoff and low infiltration rates, while the reverse leads to very good groundwater potential areas, as also reported by recent researchers [24].

In linking the geospatial findings to the geophysical survey carried out, it can clearly be observed that groundwater potential is based on structures and alluvial deposits, as prescribed earlier in this paper (Figures 3 and 8). The two-dimensional geophysical results portrayed in Figure 9 and the one-dimensional inversion charts illustrated in Appendix D agree with this statement. Structural controls related to groundwater occurrence are marked by thick downward-facing arrows (Figure 9A–F) suggesting points prone to groundwater development. Arguably, the 1-D results given in Appendix D display evidence of alluvial deposit resistivity of fresh water ranging from 10 to 100 Ωm . Other VES stations observed to have low resistivity of clay or saline nature ($>10 \Omega\text{m}$) in some layers, especially the second, third and fourth ones, with the third layer leading.

4.2. Results Validation

Validation is a crucial part of any modeled data in order to render the simulated results realistic. Past studies of a similar kind used different approaches to validate their final results. Among those which utilized borehole yields, the ones with low yields were mostly found in the poor groundwater potential zones, whereas those with high yields were located in the very good groundwater potential zones [18,40,43,45]. Others made use of the number

of dug wells or boreholes classified into perennial and non-perennial; perennial dug wells were located in very good and good groundwater potential zones, while non-perennial dug wells were found in the poor and very poor groundwater potential zones [12,21,38]. Moreover, the 1-D geophysical survey results were also used to crosscheck the delineated groundwater potential zones [22]. This approach is supported by the results of this study but with a bantam modification. In this study, however, both 1-D and 2-D results were used to analyze the GWPs with the aid of a drilled borehole. Thus, good GWPs have VES curves, with a slightly wider H-curve type signifying thick aquifer formation, with medium to relatively deeper depth; the Runzewe Mcohm profile 01 (Figure 9) and VES BKE63VES04 in Figure 8 and Appendix D are some representatives. On the contrary, the moderate to poor GWPs are matched with VES curves characterized by shallow aquifer formation, deep and narrow H-curve type and massive formations underlying the water bearing formation, as depicted by Shikalibuga and Bulangwa Mcohm profiles in Figure 7 and VESs BKE45VES01 and BKE59VES04 in Appendix D. Additionally, the borehole drilled in Nyampangwe on 24 October 2022 helped validate the delineated GWPs. Geophysical survey at that particular survey station indicated the presence of a thick aquifer at a shallow depth (~15 m), characterized by the resistivity of ~30 Ω m. Lithological logs captured during drilling period depicted the aquifer formation as partly weathered with conglomeratic deposits at depths of 20 m to 50 m, as illustrated in Figure 10. The borehole depth was 130 m and it is currently used by villagers for domestic and mining purposes.

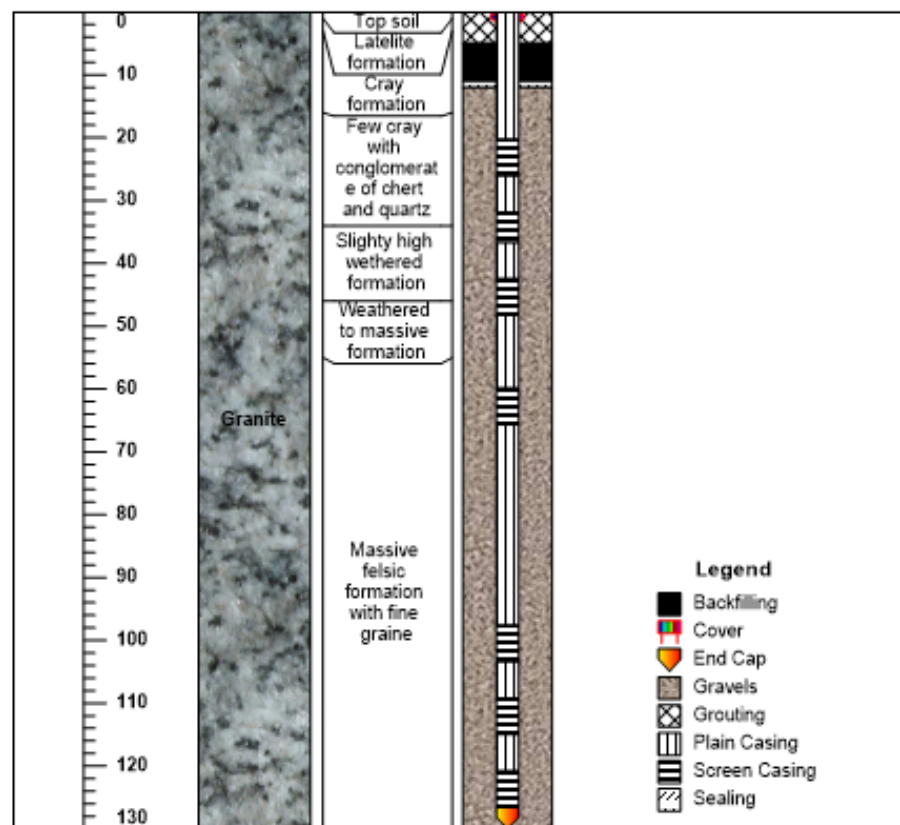


Figure 10. Nyampangwe borehole section with capacity of 20,000 L/h.

Generally, the study area is envisaged with groundwater potential in most parts, varying in depth and yield. Field experience confirms that VES curves with H-type, KH-type and HKH-type having resistivity values ranging from 10 to 100 Ω m have more than 70% of striking groundwater. This finding is supported by other research [22]. Therefore, the delineated GWPs (Figure 7b) are essential for locating other borehole sites within the study area.

5. Conclusions

The present study demonstrated that remote sensing, GIS and AHP approaches are feasible tools for demarcating GWPA in the Bukombe district, thereby providing a solid preliminary assessment for the groundwater resources in this basin, saving much money and time. Remote sensing data and conventional data were applied to compose the thematic layers that were then allocated appropriate weightage through the AHP technique. Based on the GWPA map generated, the study area was categorized into four different areas, viz., poor groundwater potential area (16.74 sq. km), moderate groundwater potential area (4104.07 sq. km), good groundwater potential area (3649.92 sq. km) and very good groundwater potential area (215.56 sq. km). Poor GWPA that cover the eastern parts of the study area can be ascribed to the accumulated influence of poor hydrogeological–environmental parameters, including low rainfall compared to the western and southern parts and the existence of hard rock regions, particularly the massive granitic rock and low lineament densities. The very good GWPA together with the good GWPA demarcated in the south, southwest and western parts of the study area are contributed to by the favorable geology (unconsolidated sediments), the low slope and drainage density, high lineament density and rainfall, and the availability of dense forest (Kigosi National Park) that favors more infiltration. The generated map is suitable for use in groundwater resources management in the Bukombe district and recommends further sites for exploration through drilling, as shown in Table 5 and Figure 11.

Table 5. Drilling sites in BD recommended for further exploration.

OBJ_ID	Latitude	Longitude	VES_No	Altitude	Village	Recommended Drilling Depth (m)
3	−3.4556	31.8800	BKE03VES2.3	1240	Katente	150
9	−3.4317	31.9017	BKE09VES1.1	1205	Bulangwa	90
11	−3.4285	31.9000	BKE11VES1.3	1202	Bulangwa	80
13	−3.4351	31.9074	BKE13VES2	1214	Bulangwa	110
22	−3.4785	31.9127	BKE22VES1.2	1208	Kapela	70
32	−3.5045	32.0315	BKE32VES04	1141	Bukombe	80
33	−3.3943	31.8662	BKE33VES01	1190	Silamila	120
36	−3.4095	31.8911	BKE36VES04	1185	Silamila	120
38	−3.4013	31.6199	BKE38VES02	1185	Msonga	100
40	−3.4010	31.6197	BKE40VES04	1177	Msonga	100
42	−3.3615	31.5613	BKE42VES02	1188	Musasa	120
44	−3.3612	31.5612	BKE44VES04	1186	Musasa	120
48	−3.5725	31.9857	BKE48VES04	1187	Iyogelo	80
49	−3.5787	31.9820	BKE49VES05	1174	Iyogelo	80
53	−3.4536	32.0685	BKE53VES03	1171	Ituga	80
54	−3.4652	32.0898	BKE54VES04	1174	Ituga	80
56	−3.4175	31.8639	BKE56VES01	1203	Butubili	120
59	−3.4151	31.8379	BKE59VES04	1199	Butubili	120
62	−3.2502	31.5967	BKE62VES03	1158	Nakayenze	100
63	−3.2477	31.5589	BKE63VES04	1150	Nakayenze	120
65	−3.4185	31.3680	BKE65VES02	1170	Ilyamchele	120
68	−3.4060	31.3977	BKE68VES05	1124	Ilyamchele	120
74	−3.3280	31.6420	BKE74VES06	1125	Nyarusunguti	80
75	−3.3285	31.6428	BKE75VES07	1118	Nyarusunguti	80
79	−3.3439	31.6403	BKE79VES04	1115	Nyampangwe	80
80	−3.3442	31.6995	BKE80VES05	1125	Nyampangwe	80
82	−3.3412	31.5301	BKE82VES02		Runzewe	60

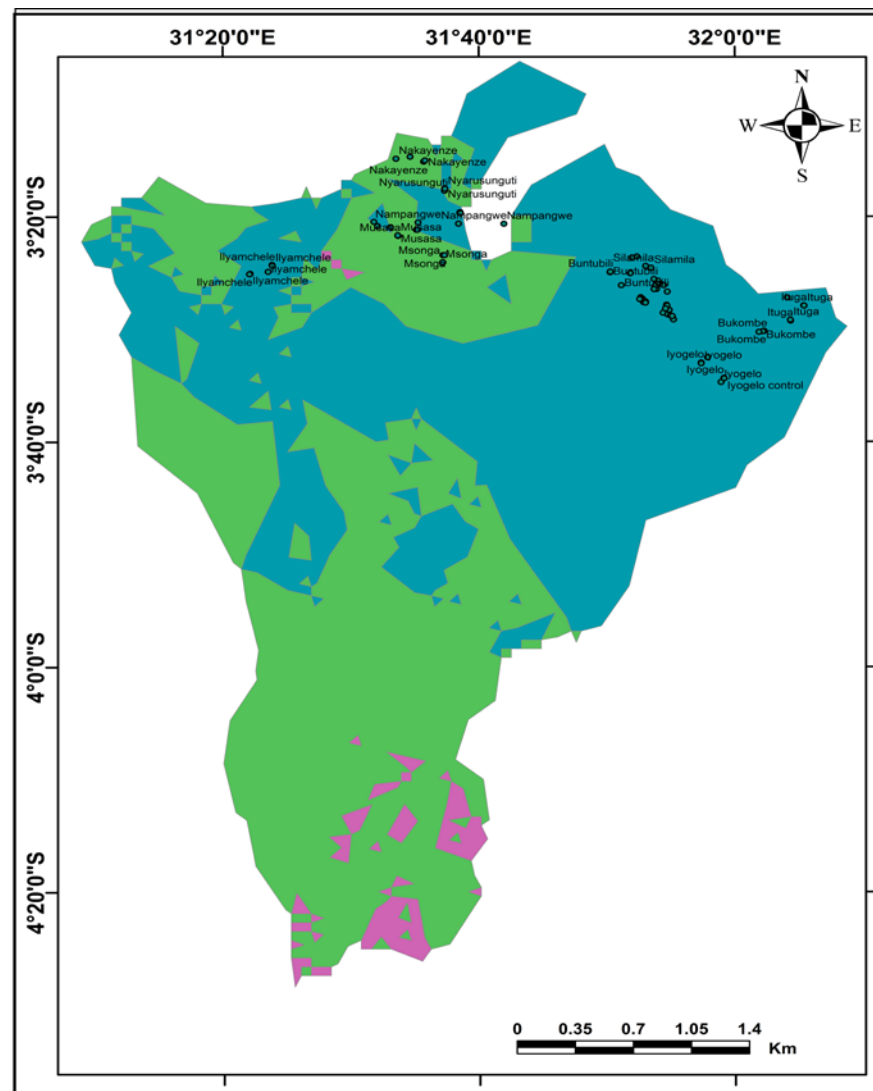


Figure 11. BD map showing VES location conducted during geophysical survey.

Author Contributions: Conceptualization, J.N.K.; methodology, J.N.K., E.E.M. and K.R.M.; software, J.N.K.; validation, J.N.K., E.E.M. and K.R.M.; formal analysis, J.N.K., E.E.M. and K.R.M.; investigation, J.N.K.; resources, J.N.K., E.E.M. and K.R.M.; data curation, J.N.K., E.E.M. and K.R.M.; writing—original draft preparation, J.N.K.; writing—review and editing, E.E.M., K.R.M. and J.N.K.; visualization, J.N.K., E.E.M. and K.R.M.; supervision, E.E.M. and K.R.M. All authors have read and agreed to the published version of the manuscript.

Funding: This research received no external funding.

Data Availability Statement: Not applicable.

Acknowledgments: This research was carried out as part of the first author's M. Sc. thesis at Sokoine University of Agriculture, Morogoro, Tanzania. The author would like to give his sincere thanks to the employer who gave permission to pursue the master program. He is also indebted to esteemed supervisors who provided suggestions and guidelines to shape the research. Lastly, the author expresses his profound sense of gratitude to the anonymous reviewers and editors for their helpful comments on the past drafts of the manuscript.

Conflicts of Interest: The authors declare that there is no conflict of interest.

Appendix A. AHP Weight Assignment during Groundwater Potential Map Development

Only input data in the light green fields and worksheets!

n=	<input type="text" value="6"/>	Number of criteria (2 to 10)	Scale: <input type="text" value="1"/>	AHP 1-9
N=	<input type="text" value="1"/>	Number of Participants (1 to 20)	α : <input type="text" value="0.1"/>	Consensus: <input type="text" value="n/a"/>
p=	<input type="text" value="1"/>	selected Participant (0=consol.)	13 7	Participant 1
Calculation of thematic weights with pairwise comparison				
Author	<input type="text" value="Goepel, C. D."/>			
Date	<input type="text"/>	Thresh: <input type="text" value="1E-08"/>	Iterations: <input type="text" value="6"/>	EVM check: <input type="text" value="3.8E-09"/>

Table	Criterion	Comment	Weights	+/-
1	Lineament density		12.8%	5.0%
2	Drainage density		4.3%	2.0%
3	Geology		29.8%	11.0%
4	LULC		8.0%	3.0%
5	Slope		4.2%	1.8%
6	Rainfall		40.8%	17.9%
7			0.0%	0.0%
8			0.0%	0.0%
9		for 9&10 unprotect the input sheets and expand the question section ("+" in row 66)	0.0%	0.0%
10			0.0%	0.0%

Result	Eigenvalue Lambda: 6.446 Consistency Ratio MRE: 41.3%	0.37 GCI: 0.26 Psi: 5.0% CR: 7.1%
---------------	-----------------------------------------------------------------------------------------------------------------------------------------------------	-----------------------------------------------------------------------------------------------------------------------------------------------------------------------------------

Matrix	Lineament density	Drainage density	Geology	LULC	Slope	Rainfall	0	0	0	0	10	normalized principal Eigenvector
Lineament density	1	5	1/4	2	4	1/5	-	-	-	-		12.83%
Drainage density	1/5	1	1/5	1/3	1	1/5	-	-	-	-		4.32%
Geology	4	5	1	5	7	1/2	-	-	-	-		29.84%
LULC	1/2	3	1/5	1	3	1/7	-	-	-	-		8.02%
Slope	1/4	1	1/7	1/3	1	1/5	-	-	-	-		4.16%
Rainfall	5	5	2	7	5	1	-	-	-	-		40.83%
0	7	-	-	-	-	-	1	-	-	-		0.00%
0	8	-	-	-	-	-	-	1	-	-		0.00%
0	9	-	-	-	-	-	-	-	1	-		0.00%
0	10	-	-	-	-	-	-	-	-	1		0.00%

Appendix B. One Dimension Geophysical Survey Results at Ilyamchele Ward, Ilyamchele Village

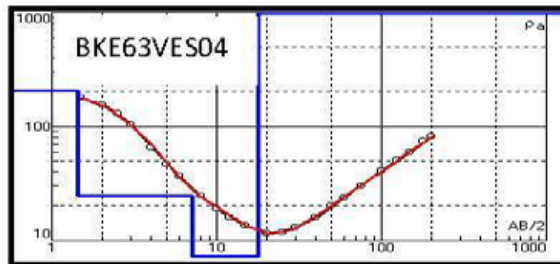
Village Region Coordinates AB/2(M)	Ilyamchele GEITA MN/2(M)	Sub-Village BKE68VES 05	Date Zone R(Ω)	District	Bukombe	
				36M K-Factor	18/04/2022 Ro_a	Alt(m)
1.5	0.5		15.024	6.28	94.351	1206
2	0.5		8.01	11.78	94.358	
2.5	0.5		4.948	18.84	93.220	
3	0.5		3.055	27.48	83.951	
4	0.5		1.306	49.46	64.595	
5	0.5		0.696	77.77	54.128	
6	0.5		0.449	112.26	50.405	
8	0.5		0.247	200.18	49.444	
10	0.5		0.153	313.22	47.923	
10		2.5	0.783	58.88	46.103	
12		2.5	0.519	86.51	44.951	
15		2.5	0.283	137.38	38.879	
20		2.5	0.106	247.28	26.212	
25		2.5	0.055	388.58	21.372	
30		2.5	0.037	561.28	20.767	
30	5		0.085	274.75	23.354	
40	5		0.046	494.55	22.749	
50	5		0.029	777.15	22.537	
50		10	0.07	376.80	26.376	
60		10	0.058	549.50	31.871	
75		10	0.044	867.43	38.167	
100		10	0.032	1554.30	49.738	
100	25		0.091	588.75	53.576	
125	25		0.071	942.00	66.882	
150	25		0.057	1373.80	78.304	
180	25			1995.50		
200	25			2472.8		

Appendix C. Rainfall Station and Their Corresponding Rainfall Reading in the Hydrological Year 2020/21 Whereby the First 19 Stations Are Records from Lake Tanganyika Basin Water Board and the Rest Two Are from Lake Victoria Basin Water Board

Station Name	Latitude	Longitude	Rainfall (mm)
Urambo Meteorology	-5.0760	32.0727	1409.1
Tabora Maji yard	-5.0070	32.7387	1019.6
Sikonge Meteorology	-5.6268	32.7563	1066.1
Uyowa Meteorology	-4.7830	32.0690	993.3
Kazima Dam	-5.0076	32.9144	655
Lumbe Meteorology	-5.5000	31.4833	1102.3
Ushetu Meteorology	-4.1667	32.0167	895.7
Kagera Nkanda Meteorology	-4.5821	30.5817	1136.1
Kigoma Maji yard	-4.9000	29.6500	1037.9
Kahama Meteorology	-3.8229	32.5893	997.3
Kibondo Meteorology	-3.5795	30.7165	1205.1
Igombe Dam	-4.9002	32.7139	1107.2
Uvinza Meteorology	-5.0970	30.3859	952.1
Kasanga Meteorology	-8.4639	31.1393	503.9
Masolo Primary School	-7.7910	31.0064	699.3
Nguruka Meteorology	-5.1667	31.0833	1885.5
Janda	-4.6059	29.8765	1451.6
Karema	-6.7500	30.4167	771
Ushiroombo Meteorology	-3.4594	31.8909	987.3
Magufuli	-3.0386	31.7418	1171.2
Biharamulo	-2.6318	31.3030	710.6

Appendix D. VES Curves and Their Resistivity Tables

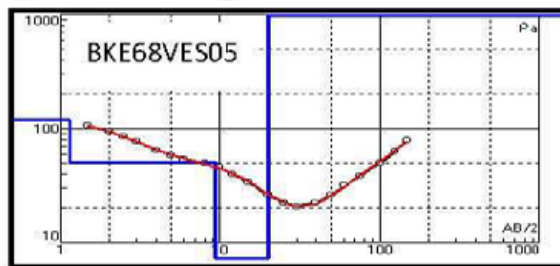
Nakayenze Village BKE63VES04



RDD 120m

N	ρ	h	d	Alt
1	207.5	1.439	1.439	-1.439
2	24.52	5.623	7.062	-7.062
3	4.786	10.66	17.72	-17.722
4	8199			

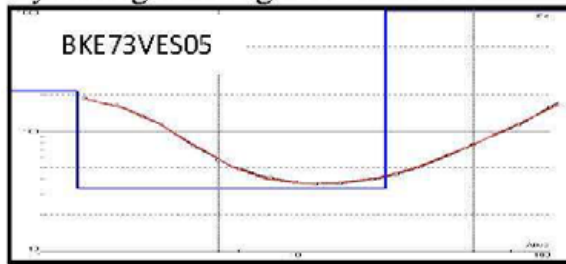
Iyamchele Village BKE68VES05



RDD 120m

N	ρ	h	d	Alt
1	120.8	1.143	1.143	-1.143
2	50.61	8.284	9.427	-9.427
3	6.08	10.7	20.13	-20.127
4	12915			

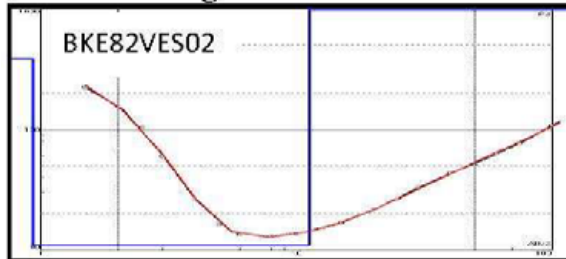
Nyalusunguti Village BKE73VES05



RDD 60m

N	ρ	h	d	Alt
1	217	1.4	1.4	-1.403
2	33.3	21.2	22.6	-22.63
3	32246			

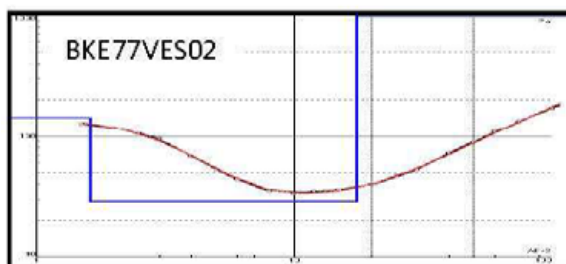
Runzewe Village BKE82VES02



RDD 80m

N	ρ	h	d	Alt
1	384	0.932	0.932	-0.9323
2	11	10.3	11.2	-11.24
3	18352			

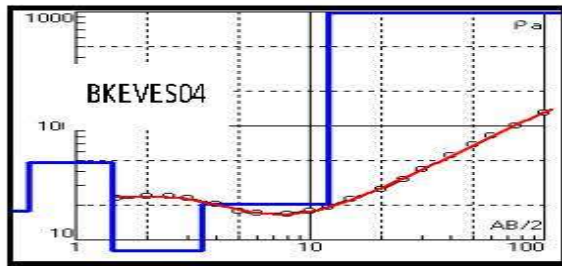
Nyampangwe Village BKE77VES02



RDD 50m

N	ρ	h	d	Alt
1	143	1.62	1.62	-1.618
2	28.7	15.9	17.5	-17.48
3	12038			

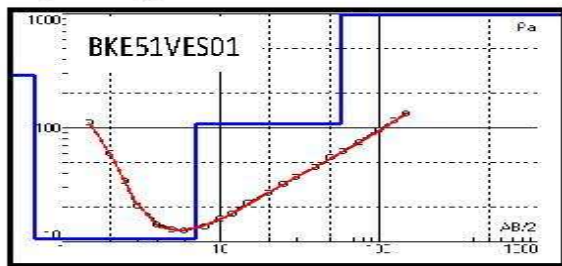
Bukombe Village BKE30VES02



RDD 50m

N	ρ	h	d	Alt
1	17.99	0.6351	0.6351	-0.6351
2	47.7	0.7906	1.426	-1.426
3	8.044	2.004	3.43	-3.429
4	20.39	8.54	11.97	-11.9
5	2308			

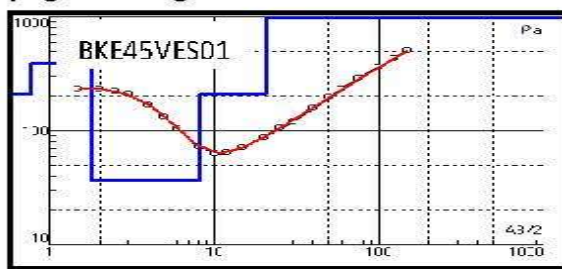
Ituga Village BKE51VES01



RDD 70m

N	ρ	h	d	Alt
1	288.7	0.6708	0.6708	-0.6708
2	10.61	6.373	7.044	-7.043
3	109.4	50.47	57.51	-57.51
4	2104			

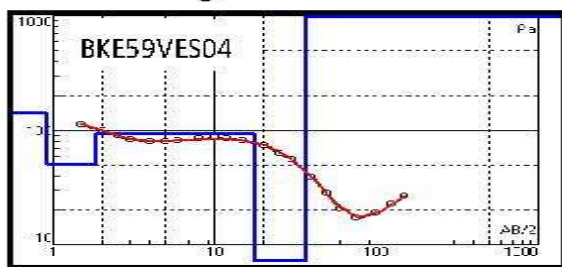
Iyogelo Village BKE45VES01



RDD 20m

N	ρ	h	d	Alt
1	209.9	0.7783	0.7783	-0.7783
2	387.3	1.012	1.79	-1.790
3	36.76	6.37	8.16	-8.160
4	211.5	12.4	20.56	-20.56
5	2292			

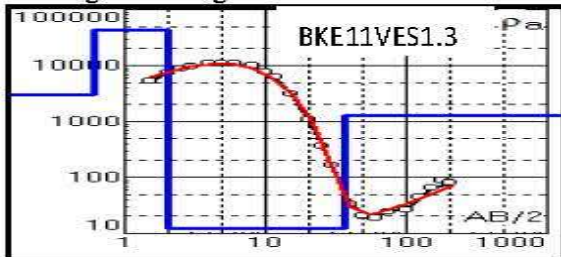
Buntubili Village BKE59VES04



RDD 120m

N	ρ	h	d	Alt
1	144.6	0.8974	0.8974	-0.8974
2	50.49	0.9404	1.838	-1.8378
3	93.89	15.85	17.69	-17.688
4	3.515	18.73	36.42	-36.418
5	2652			

Bulangwa Village BKE11VES1.3



RDD 130m

N	ρ	h	d	Alt
1	2995	0.60733	0.60733	0.60733
2	43071	1.4298	2.0371	2.0371
3	12.331	34.721	36.758	36.758
4	1296			

Appendix E. Weights of Individual Thematic Layers and Their Respective Class Feature Ranks (Adopted and Modified from Nilawar 2014)

Theme	Weight (%)	Class Interval	Class Description	Groundwater Potentiality	Rank
LULC	8		Built up	Very Poor	1
			Water body	Medium	3
			Vegetation	Very Good	5
			Agricultural land	Good	4
			Bare land	Poor	2
Lineaments density (km/sq. km)	12.8	0–6	Very low	Very Poor	1
		6–15	Low	Poor	2
		15–27	Medium	Medium	3
		27–42	High	Good	4
		42–68	Very High	Very Good	5
Drainage Density (km/sq. km)	4.3	0–35.33	Very low	Very Good	5
		5.33–15.72	Low	Good	4
		15.72–26.95	Medium	Medium	3
		26.95–40.98	High	Poor	2
		40.98–71.58	Very High	Very Poor	1
Slope (%)	4.2	0–2.7	Very low	Very Good	5
		2.8–4.9	Low	Good	4
		5.0–7.5	Medium	Medium	3
		7.6–11	High	Poor	2
		12–42	Very High	Very Poor	1
Geology	29.8	Granite and syenites Bukoban System Nyanzian System	migmatites, plutonics and orphyrites	Very Poor	1
				Poor	2
				Poor	2
		Metasedments	BIF and Ferruginous schist, gneiss, phyllites, quartzite, amphibolite and marble	Moderate	3
		Alluvial deposit	Alluvial deposit	Very Good	5
Rainfall (mm/year)	40.8	Recent Marine to terrestrial sediments	clay, calcrete, limestone, silicrete, silt, gravels, sand	Good	4
		Volcanic lava	Basalt		3
		1013–1043	Very low	Very Poor	1
		1044–1068	Low	Poor	2
		1069–1091	Medium	Medium	3
	1092–1123	High	Good	4	
	1124–1171	Very High	Very Good	5	

References

- UNICEF. *Meeting the MDG Drinking Water and Sanitation Target. A Mid-Term Assessment of Progress*; UNICEF: New York, NY, USA, 2004.
- Mjemah, I.C.; van Camp, M.; Martens, K.; Walraevens, K. Groundwater exploitation and recharge rate estimation of a quaternary sand aquifer in Dar-es-Salaam area, Tanzania. *Environ. Earth Sci.* **2011**, *63*, 559–569. [[CrossRef](#)]
- Mahoo, H.; Simukanga, L.; Kashaga, R.A.L. Water Resources Management in Tanzania: Identifying Research Gaps and Needs and Recommendations for a Research Agenda. *Tanzan. J. Agric. Sci.* **2015**, *14*, 57–77.
- Makoba, E.; Muzuka, A.N.N. Water quality and hydrogeochemical characteristics of groundwater around Mt. Meru, Northern Tanzania. *Appl. Water Sci.* **2019**, *9*, 120. [[CrossRef](#)]
- Oiro, S.; Comte, J.C.; Soulsby, C.; McDonald, A.; Mwakamba, C. Depletion of groundwater resources under rapid urbanisation in Africa: Recent and future trends in the Nairobi Aquifer System, Kenya. *Hydrogeol. J.* **2020**, *28*, 2635–2656. [[CrossRef](#)]
- Mussa, K.R.; Mjemah, I.C.; Walraevens, K. Quantification of groundwater exploitation and assessment of water quality risk perception in the Dar Es Salaam quaternary aquifer, Tanzania. *Water* **2019**, *11*, 2552. [[CrossRef](#)]
- Duan, H.; Deng, Z.; Deng, F.; Wang, D. Assessment of groundwater potential based on multicriteria decision making model and decision tree algorithms. *Math. Probl. Eng.* **2016**, *2016*, 1–12. [[CrossRef](#)]
- Todd, D.K.; Mays, L.W. *Groundwater Hydrology*; Wiley: New York, NY, USA, 2004.
- UNICEF. *2015 Update and MDG Assessment*; UNICEF: New York, NY, USA, 2015.
- Anteneh, Z.L.; Alemu, M.M.; Bawoke, G.T.; Kehali, A.T.; Fenta, M.C.; Desta, M.T. Appraising groundwater potential zones using geospatial and multi-criteria decision analysis (MCDA) techniques in Andasa-Tul watershed, Upper Blue Nile basin, Ethiopia. *Environ. Earth Sci.* **2021**, *81*, 1–37. [[CrossRef](#)]

11. Bakundukize, C.; Mtoni, Y.; Martens, K.; Van Camp, M.; Walraevens, K. Poor understanding of the hydrogeological structure is a main cause of hand-dug wells failure in developing countries: A case study of a Precambrian basement aquifer in Bugesera region (Burundi). *J. Afr. Earth Sci.* **2016**, *121*, 180–199. [[CrossRef](#)]
12. Ally, A.M.; Mayunga, S.D. Identification of Potential Groundwater Zones in Semi-Arid Areas: A Case Study of Bahi District—Central Tanzania. *Int. J. Eng. Sci. Innov. Technol. IJESIT* **2019**, *8*, 8–20.
13. Olorunfemi, M.O.; Oni, A.G. Integrated geophysical methods and techniques for siting productive boreholes in basement complex terrain of southwestern Nigeria. *Ife J. Sci.* **2019**, *21*, 13. [[CrossRef](#)]
14. Elisante, E.; Muzuka, A.N.N. Occurrence of nitrate in Tanzanian groundwater aquifers: A review. *Appl. Water Sci.* **2017**, *7*, 71–87. [[CrossRef](#)]
15. The Ministry of Water. Tanzania Water Resources Atlas. Ministry Website. 2019. Available online: https://www.maji.go.tz/uploads/publications/TWRA_F.pdf (accessed on 25 January 2023).
16. SMEC. *Integrated Water Resources Management and Development Plans for Lake Tanganyika Basin Water Board*; SMEC: Dar es Salaam, Tanzania, 2015.
17. Shemsanga, C.; Martz, A.N.N.M.L.; Mcharo, H.K.E. Indigenous knowledge on development and management of shallow dug wells of Dodoma Municipality in Tanzania. *Appl. Water Sci.* **2018**, *8*, 1–20. [[CrossRef](#)]
18. Nsiah, E.; Appiah-adjei, E.K.; Adjei, K.A. Hydrogeological delineation of groundwater potential zones in the Nabogo basin, Ghana. *J. African Earth Sci.* **2018**, *143*, 1–9. [[CrossRef](#)]
19. Rwebugisa, R.A. Groundwater Recharge Assessment in the Makutupora Basin, Dodoma Tanzania. Master's Thesis, International Institute for Geo-Information Science and Earth Observation, Enschede, The Netherlands, 2008.
20. Kumar, P.; Herath, S.; Avtar, R.; Takeuchi, K. Mapping of groundwater potential zones in Killinochi area, Sri Lanka, using GIS and remote sensing techniques. *Sustain. Water Resour. Manag.* **2016**, *2*, 419–430. [[CrossRef](#)]
21. Ahmed, K.; Shahid, S.; Bin Harun, S.; Ismail, T.; Nawaz, N.; Shamsudin, S. Assessment of groundwater potential zones in an arid region based on catastrophe theory. *Earth Sci. Inform.* **2015**, *8*, 539–549. [[CrossRef](#)]
22. Allafta, H.; Opp, C.; Patra, S. Identification of groundwater potential zones using remote sensing and GIS techniques: A case study of the shatt Al-Arab Basin. *Remote Sens.* **2020**, *13*, 112. [[CrossRef](#)]
23. Murasingh, S. Analysis of Groundwater Potential Zones Using Electrical Resistivity, Rs & Gis Techniques in a Typical Mine Area of Odisha. Master's Thesis, National Institute of Technology, Rourkela, India, 2014. [[CrossRef](#)]
24. Andualem, T.G.; Demeke, G.G. Groundwater potential assessment using GIS and remote sensing: A case study of Guna tana landscape, upper blue Nile Basin, Ethiopia. *J. Hydrol. Reg. Stud.* **2019**, *24*, 100610. [[CrossRef](#)]
25. United Republic of Tanzania. *National Population Projections*; 2018. Available online: <https://www.nbs.go.tz/nbs/takwimu/census2012/Projection-Report-20132035.pdf> (accessed on 25 January 2023).
26. DC, B. bukombe utawala na utumishi _ BUKOMBE DISTRICT COUNCIL. 2021. Available online: <http://www.bukombedc.go.tz/utawala-na-utumishi> (accessed on 25 January 2023).
27. TMA. *Statement on the Status of Tanzania Climate in 2020*; TMA: Dodoma, Tanzania, 2020.
28. Henckel, J.; Poulsen, K.H.; Sharp, T.; Spora, P. Lake Victoria goldfields. *Epis. J. Int. Geosci.* **2016**, *39*, 135–154. [[CrossRef](#)]
29. Barth, A.H. Barth 1990 Provisional Geo Map of Lake Victoria Gold Fields.pdf. 1990. Available online: <https://www.schweizerbart.de> (accessed on 25 January 2023).
30. Taylor, M.J. *Report on the Ushiroambo Mineral Exploration Property of Tanzanian Royalty Exploration Corporation in the Bukombe District, Shinyanga Region of the United Republic of Tanzania, East Africa*; Hindawi Publisher: Toronto, Canada, 2009.
31. Joel, E.S.; Olasehinde, P.I.; Adagunodo, T.A.; Omeje, M.; Oha, I.; Akinyemi, M.L.; Olawole, O.C. Geo-investigation on groundwater control in some parts of Ogun state using data from Shuttle Radar Topography Mission and vertical electrical soundings. *Heliyon* **2020**, *6*, e03327. [[CrossRef](#)]
32. Bouderbala, A.; Remini, B.; Hamoudi, A.S. Geoelectrical investigation of saline water intrusion into freshwater aquifers: A case study of Nador coastal aquifer, Tipaza, Algeria. *Geofísica Int.* **2016**, *55*, 239–253. [[CrossRef](#)]
33. Harist, M.C.; Afif, H.A.; Putri, D.N.; Putut, I.; Shidiq, A. GIS modelling based on slope and morphology for landslide potential area in Wonosobo, Central Java. *MATEC Web Conf.* **2018**, *03004*, 1–6. [[CrossRef](#)]
34. Congedo, L. Semi-Automatic Classification Plugin Documentation. 2020. Available online: <https://www.youtube.com/watch?v=Ceyhm3DZINY> (accessed on 25 January 2023).
35. Das, S. Extraction of lineaments from different azimuth angles using geospatial techniques: A case study of Pravara basin, Maharashtra, India. *Arab. J. Geosci.* **2018**, *11*, 1–13. [[CrossRef](#)]
36. Goepel, K.D. BPMSG AHP Excel Template with Multiple INPUTS. Available online: <http://bpmsg.com> (accessed on 25 January 2023).
37. Patra, S.; Mishra, P.; Mahapatra, S.C. Delineation of groundwater potential zone for sustainable development: A case study from Ganga Alluvial Plain covering Hooghly district of India using remote sensing, geographic information system and analytic hierarchy process. *J. Clean. Prod.* **2018**, *172*, 2485–2502. [[CrossRef](#)]
38. Roy, S.; Hazra, S.; Chanda, A.; Das, S. Assessment of groundwater potential zones using multi-criteria decision-making technique: A micro-level case study from red and lateritic zone (RLZ) of West Bengal, India. *Sustain. Water Resour. Manag.* **2020**, *6*, 1–14. [[CrossRef](#)]
39. Makoba, E.; Muzuka, A.N.N. Delineation of groundwater zones with contrasting quality in the fluorotic zone, around Mount Meru, northern Tanzania. *Hydrol. Sci. J.* **2021**, *66*, 322–346. [[CrossRef](#)]

40. Kaliraj, S.; Chandrasekar, N.; Magesh, N.S. Identification of potential groundwater recharge zones in Vaigai upper basin, Tamil Nadu, using GIS-based analytical hierarchical process (AHP) technique. *Arab. J. Geosci.* **2014**, *7*, 1385–1401. [[CrossRef](#)]
41. Lakshmi, V.; Reddy, V.K. Identification of Groundwater Potential Zones using GIS and Remote Sensing. *Int. J. Pure Appl. Math.* **2018**, *119*, 3195–3210.
42. Mkumbo, N.J.; Mussa, K.R.; Mariki, E.E. The Use of the DRASTIC-LU/LC Model for Assessing Groundwater Vulnerability to Nitrate Contamination in Morogoro Municipality, Tanzania. *Earth* **2022**, *3*, 1161–1184. [[CrossRef](#)]
43. Manap, M.A.; Sulaiman, W.N.A.; Ramli, M.F.; Pradhan, B.; Surip, N. A knowledge-driven GIS modeling technique for groundwater potential mapping at the Upper Langat Basin, Malaysia. *Arab. J. Geosci.* **2011**, *6*, 1621–1637. [[CrossRef](#)]
44. Waikar, M.L.; Nilawar, A.P. Identification of Groundwater Potential Zone using Remote Sensing and GIS Technique. *Int. J. Innov. Res. Sci. Eng. Technol.* **2014**, *3*, 12163–12174.
45. Rahmati, O.; Nazari Samani, A.; Mahdavi, M.; Pourghasemi, H.R.; Zeinivand, H. Groundwater potential mapping at Kurdistan region of Iran using analytic hierarchy process and GIS. *Arab. J. Geosci.* **2015**, *8*, 7059–7071. [[CrossRef](#)]
46. Fetter, C.W. *Applied Hydrogeology*; Prentice-Hall, Inc.: Upper Saddle River, NJ, USA, 2001.
47. Gintamo, T.T. Ground Water Potential Evaluation Based on Integrated GIS and Remote Sensing Techniques, in Bilate River Catchment: South Rift Valley of Ethiopia. *Am. Sci. Res. J. Eng. Technol. Sci.* **2015**, *10*, 85–120.
48. Mussa, K.R.; Mjemah, I.C.; Machunda, R.L. Open-Source Software Application for Hydrogeological Delineation of Potential Groundwater Recharge Zones in the Singida Semi-Arid, Fractured Aquifer, Central Tanzania. *Hydrology* **2020**, *7*, 28. [[CrossRef](#)]

Disclaimer/Publisher’s Note: The statements, opinions and data contained in all publications are solely those of the individual author(s) and contributor(s) and not of MDPI and/or the editor(s). MDPI and/or the editor(s) disclaim responsibility for any injury to people or property resulting from any ideas, methods, instructions or products referred to in the content.